Thermorph: Democratizing 4D Printing of Self-Folding Materials and Interfaces

Byoungkwon An[1,2*], Ye Tao[1,3*], Jianzhe Gu[1], Tingyu Cheng[1], Xiang 'Anthony' Chen[1], Xiaoxiao Zhang[4], Wei Zhao[5], Youngwook Do[1], Shigeo Takahashi[6], Hsiang-Yun Wu[7], Teng Zhang[4], Lining Yao[1]

[1]Carnegie Mellon University, [2]Duke University, [3]Zhejiang University, [4]Syracuse University, [5]Glodon Company Limited, [6]University of Aizu, [7]TU Wien

[1]{byoungka, ytao2, jianzheg, tcheng1, xiangche, hyoungwd, liningy}@cs.cmu.edu, [3]taoye@zju.edu.cn, [4]{xzhan150, tzhang48}@syr.edu, [5]zhaow-j@glodon.com, [6,7]{takahashis, hsiang.yun.wu}@acm.org

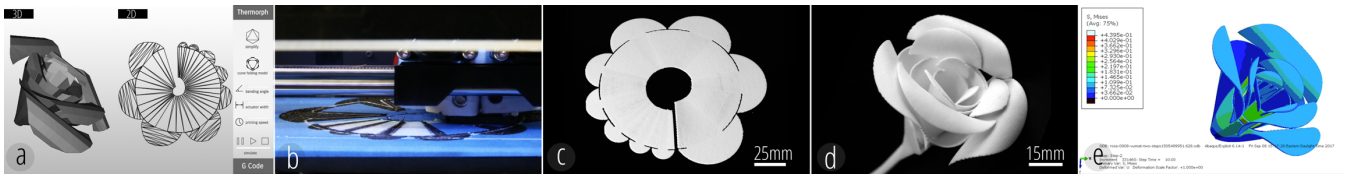

Figure 1. Thermorph overview. (a) Design editor to define and simulate the self-folding composite; (b) the printing toolpath of a flat sheet is generated from (a) and printed on an FDM printer; (c) the printed flat sheet; (d) the flat sheet self-folds sequentially into a rose; (e) finite element based simulation of the self-folding rose to verify our hypothesis on the material mechanism.

ABSTRACT

We develop a novel method printing complex self-folding geometries. We demonstrated that with a desktop fused deposition modeling (FDM) 3D printer, off-the-shelf printing filaments and a design editor, we can print flat thermoplastic composites and trigger them to self-fold into 3D with arbitrary bending angles. This is a suitable technique, called Thermorph, to prototype hollow and foldable 3D shapes without losing key features. We describe a new curved folding origami design algorithm, compiling given arbitrary 3D models to 2D unfolded models in G-Code for FDM printers. To demonstrate the Thermorph platform, we designed and printed complex self-folding geometries (up to 70 faces), including 15 self-curved geometric primitives and 4 self-curved applications, such as chairs, the simplified Stanford Bunny and flowers. Compared to the standard 3D printing, our method saves up to 60% - 87% of the printing time for all shapes chosen.

Author Keywords

3D printing; 4D printing; shape memory polymer; thermoplastic; self-folding; shape changing; computational geometry; computational fabrication.

ACM Classification Keywords

H.5.m. Information Interfaces and Presentation: User Interfaces;

INTRODUCTION

3D Printing is still slow to complete the printing of reasonably sized 3D objects [21]. The rose flower in Figure 2a takes almost 9 hours to be printed on our FDM printer (MakerBot Replicator 2X), and requires at least 15 minutes for post processing. Recently, researchers have devised many ways to speed up the 3D printing and prototyping processes, including replacing non-critical parts with low-fidelity structures [19, 21, 34], inventing new solidification mechanisms [37] and machine control mechanisms [40]. Self-folding materials have been mentioned as one way to increase the speed of manufacturing 3D objects. However, the previous methods require intensive laser stacking and a post-assembly process [1, 8, 14, 36]. To automate the making of self-folding and transforming materials, researchers investigated printing processed and coined 4D printing methods [35]. However, even for 4D printed self-folding materials, challenges exist for their general accessibility: either these systems require material synthesized by someone with expertise in material science or chemistry [11, 12], or the material is not generalized enough to be used to create certain arbitrary 3D geometries [28].

Due to the obvious advantage of the self-folding process to accelerate the fast prototyping of 3D objects, as well as the progress and constraints in the previous self-folding related projects, we feel the urge to bring self-folding materials and mechanisms further and present them to the HCI

∗The first two authors contributed equally to this work.

CHI 2018, April 21–26, 2018, Montreal, QC, Canada

ACM 978-1-4503-5620-6/18/04...$15.00
https://doi.org/10.1145/3173574.3173834

community as an example of a practical and fast prototyping technique. Thermorph is to fulfill this mission (Figure 1).

To make it a practical platform, there were a few criteria we set as Thermorph was developed:

- It should be an automated printing process, no pre- or post-processing.
- It should be on a desktop FDM printer to make this 4D printing technique readily accessible for researchers, hobbyists, classrooms, museums and developing countries.
- It should use off-the-shelf, low-cost and accessible printing filaments.
- While heat is generated by various energy sources and is deliberated by various media, such as air, microwave or water [12, 28, 45], Thermorph should be made of thermoplastic for its fitness as a general prototyping material.
- Thermorph should be an end-to-end approach, which means that users can input their desired 3D shape and see the printer printing it out automatically.
- Unlike most of the self-folding and 4D printing work which showcases a group of predesigned primitives and combinations of these primitives, Thermorph should be able to handle arbitrary 3D geometries.

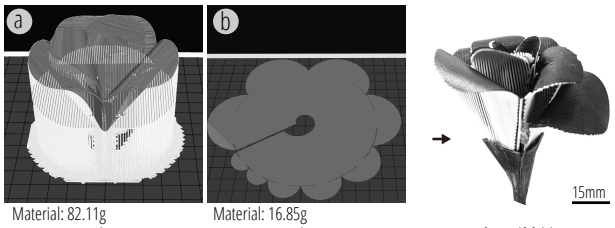

Figure 2. A comparison of the estimate of the printing time and material consumption. (a) 3D model of a rose printed in the standard mode; and (b) flat Thermorph composite which can self-folds into the same rose as (a) after being heated.

Figure 2 shows the estimate of the printing time and material consumption from Makebot Print, the official slicing software for commercial desktop 3D Printer MakerBot. Figure 2a is a 3D model of a rose printed normally. Figure 2b is a Thermorph flat composite that consists of four layers; it self-folds into a rose with the same size as the first one when heated. Comparing the Thermorph approach with the standard FDM 3D printing approach, to print out the same rose, Thermorph saves 86% printing time, 75% printing materials and 99% post processing time.

In this paper, we firstly describe the material mechanism, and demonstrate a library of primitives. We then walk through our software to demonstrate its design capability, followed by the implementation of its pipeline. Lastly, we describe application prototypes in the context of self-folding furniture, transportation, armors and decorative art.

CONTRIBUTIONS AND LIMITATIONS

The main contributions of the work are as follows:

- Novel material composite and printing method: we present a novel way of creating self-folding composite structures with easily accessible FDM printers and off-the-shelf thermoplastic printing filaments. The unique composite design and printing method enable a programmable bending angle ranging from -180° to 180°, and a wide range of geometrical primitives.
- Automated design and fabrication pipeline: our prior work [1] showed a pipeline to handle arbitrary 3D geometries with sharp folds. In this paper, we extend and generalize the pipeline by developing new modules, including a design algorithm for curved origami (self-folding) geometries and web-based user-interface software.
- We implement several application scenarios that demonstrate the use of Thermorph: self-folding furniture, boats, armors, and decorative art pieces.

However, the resulting techniques are also subject to limitations:

- The constraints of printing size and resolution with standard desktop FDM printers, the suitable shapes are 3D meshes that can be simplified into a limited number (< 70) of flat faces without losing key features. Based on our experiments, a shape with no more than 40 faces can be printed with a good quality on a Makerbot Replicator 2X with a 25x15cm printing capacity. This step is optional for a directly printable mesh.
- Our simulation tool does not consider gravity and the material's own weight. For most of the complex shapes shown in the application section, we fold them up in a heated water tank to attenuate the effect of weight, and we chose the relatively centered face as the fixed face during the folding process, or purposely modified the printing speed from the theoretical calculation to mitigate gravity influence. Currently, our material can fold in mid-air but the transformation cannot be simulated precisely with our software.
- The structure has small holes at the end of each hinge, which is due to the inherent constraints of the unfolding algorithms we use (Figure 12).

BACKGROUND: SHAPE MEMORY OF THERMOPLASTIC

Shape memory thermoplastic has the capability of changing its shape upon temperature changes [43]. The shape memory effect exists in a large group of thermoplastics, including widely-used PLA and ABS in FDM 3D printing.

There are two important temperature parameters to study shape memory thermoplastic: glass transition temperature (T_g) and melting temperature (T_m) which control the phase transitions of the plastic (Figure 3). For our Thermorph material which contains shape memory PLA, we have to heat it above its T_g (60-65℃) and below its T_m (173-178℃) in order to make it elastic and trigger it to self-fold.

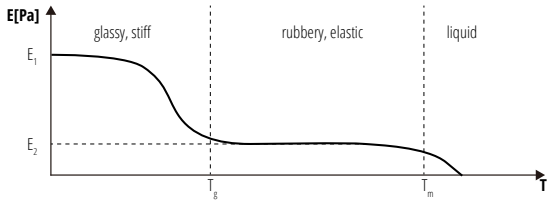

Figure 3. State transitions of thermoplastics: stiffness versus heating temperature.

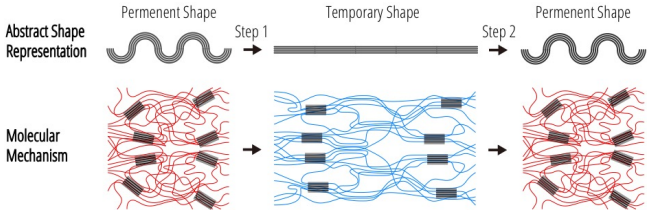

Figure 4. Molecular mechanism in a two-step shape memory effect.

As Figure 4 shows that shape memory process consists of two steps. *Step 1 - shape programming*: we can heat a thermoplastic above its T_g and below its T_m to mold it from its original shape (permanent shape) into a temporary shape, and keep it at its temporary shape by decreasing the temperature below T_g; *Step 2 - shape recovery*: the temporary shape can turn back to its permanent shape if we reheat the material to be above T_g [17]. In the next section, we will talk about how Thermorph material is designed by utilizing this effect.

THERMORPH MATERIALS

Mechanisms of Thermorph Material

During the printing process, the polymer chain is being rearranged and *residual stress* can be built: when PLA is being extruded, the polymer chain is pulled and straight; it will be forced to keep the straight state (the state of Temporary Shape after Step 1 in Figure 4) after it quickly cools and solidifies. If we reheat the solidified PLA, it will release the *residual stress,* return its polymer chain to its chaotic, or low energy mode, and shorten along the printing direction (the state of Permanent Shape after Step 2 in Figure 4).

In order to convert this shortening effect upon reheating into a bending behavior for our self-folding purpose, we propose a bi-layer structure: one layer of Thermopolyurethane (TPU) as the *constrain layer* and three layers of PLA as the *active layer*. Together these four layers form an actuator.

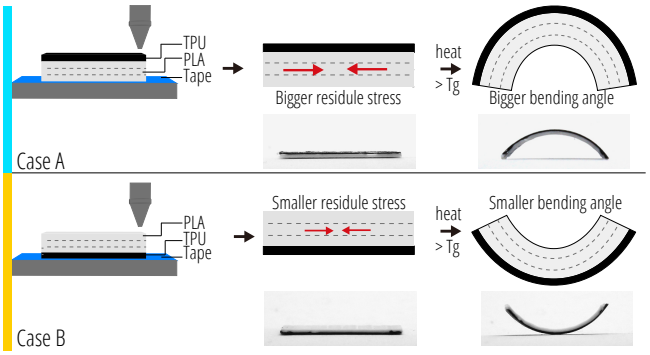

Figure 5. Two printing orders of Thermorph material cause different bending directions and angles. Case A is with PLA layer (the *active layer*) printed firstly at the bottom; case B is with TPU layer (the *constrain layer*) printed firstly.

Figure 5 shows two possible ways of printing Thermorph actuator to achieve both concave and convex folding. In case A, the PLA layer is printed firstly; and in case B, the TPU layer is printed firstly. Both cases can bend substantially upon being heated. However, case A has a bigger bending angle than case B. That is because that the *active layer* (the PLA layer) in case A is printed on a relatively cool substrate - blue tape on the printing bed, while case B has its *active layer* (the PLA layer) printed on a comparably warm substrate - the previous TPU layer. As a result, PLA in case A built a bigger residual strain/stress comparing with case B.

Moreover, the different bending angles in both cases are due to another reason: the differences in the residual stress between the top and bottom sides of one single PLA layer. Upon heating, the bottom side shrinks more as it retains more stress due to the constraints of the printing bed or the existing layer below [3, 31]. As a result, one single PLA layer tends to bend downwards when reheated. In case A, both the stress in each single PLA layer and the global constrains of TPU cause the strip to bend downwards, thus both effects add up for a downward bending; however, in case B, two effects cause opposite bending directions, and so the final behaved bending angle is smaller than case A.

Controllability

We conducted a quantitative analysis of the bending performance on both actuators (case A and B from Figure 5). All the samples contain a middle actuator part and two side face parts. The *fold angle* of a sample is defined by an excluded angle of the extension lines from two side faces (the excluded angle is 180° minus the included angle). As explained before, the *actuator* part is composed of three *active layers* (PLA) and one *constrain layer* (TPU). We measured how the printing speed (Figure 6) and the length of the actuator (Figure 7) can affect the bending angle for both cases. The data is used to provide us not only a reference for the design, but also a quantitative material performance guideline for the software development.

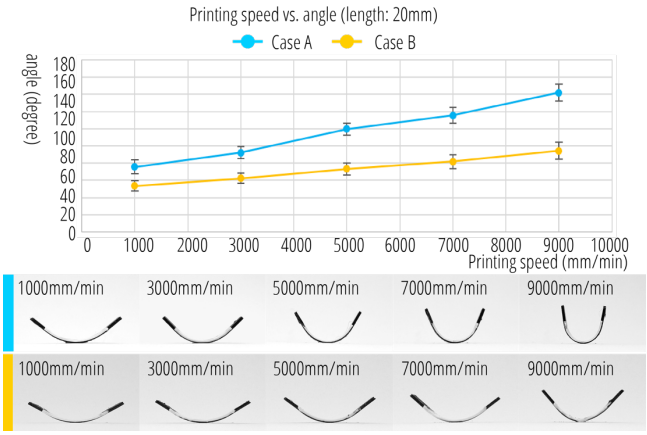

Figure 6. The fold angle as a function of the printing speed of the PLA layers (the length and width of the PLA is 20mm and 10mm, respectively). The printing speed of the TPU was 1500mm/min.

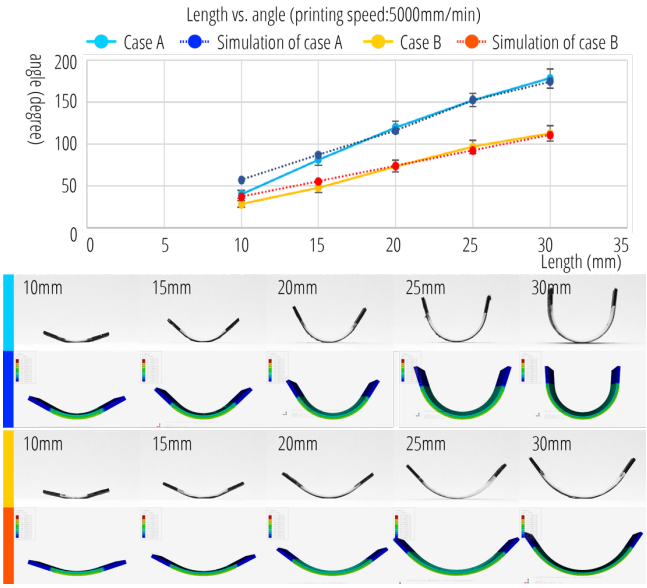

Figure 7. The fold angle as a function of the actuator length (the width of each sample is 10mm). The printing speed of the TPU was 1500mm/min, PLA was 5000mm/min.

Figure 6 shows that as the printing speed of the PLA layers is increased, the fold angle increases as well. This can be intuitively understood as that the faster the printing filament is pulled, the larger the residual stress is formed within the printing filament, and the more dramatically it will recover.

Figure 7 shows that the length of the actuator can be another very effective parameter to tune the bending angle. The bending angles measured for case A and B are used as a reference in our Thermorph editor discussed in the following section. In addition to the experimental results, we have performed a finite element analysis based simulation to verify our experiments and hypothesis on the material mechanisms. Figure 7 shows that the simulation is well aligned with the experimental data.

THE DESIGN PRIMITIVES OF THERMORPH

Geometrical Primitives

By controlling the printing orientation and printing speed of the *active layer* (PLA) within the actuator, we can create a wide variety of geometrical shapes that can be folded from flat patterns (see Table 1 at the end of the paper).

For all the samples except those under the *polyhedron fold* category, we can plan the printing toolpath with the forward design flow in our software editor (explained in the following section); all the samples of *polyhedron fold* are designed with the inverse design flow by importing the desired 3D models.

PLA and TPU were extruded through a 0.4mm nozzle. PLA was heated to 210 °C and TPU 230 °C. Layer thickness was 0.2mm. All the printed samples were triggered at 70 °C for ~2 minutes for their self-folding effects.

Straight Fold: the printing lines of the actuator are parallel to at least one of the geometry edges.

Angled Fold: the printing lines of the actuator are not parallel to any geometry edges.

Two-side Fold: actuator layers are located on both sides of the geometry.

Circular Fold: the printing lines of the actuator are circular. Compared to some other thermoplastic based self-folding techniques [1, 18], our technique has an advantage of printing curved creases with ease and flexibility.

Polygonal Fold: lines fold into polygons. The narrow actuator is achieved by increasing the printing speed from commonly recommended PLA printing speed of 3000 mm/min to 9000 mm/min.

Polyhedron Fold: we showed a series of polyhedrons with printing tool path produced by our software tool. These were generated and printed quickly, with 15 - 30 minutes designing and printing time for each.

Shape Memory Primitives

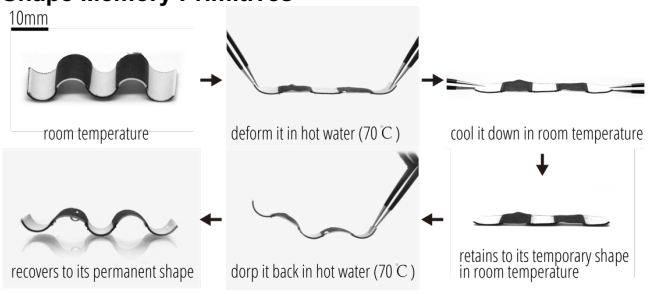

Figure 8. Shape recovery effect.

All the self-folding structures printed here retain the shape memory effect introduced in previous Figure 4. If we deform the folded shape under heat, it can recover to its folded state (Figure 8). This repetitive deforming-recovering effect can be utilized for interaction design, such

as the iron deformable armor we discussed in the application (Figure 17).

THERMORPH USER INTERFACE

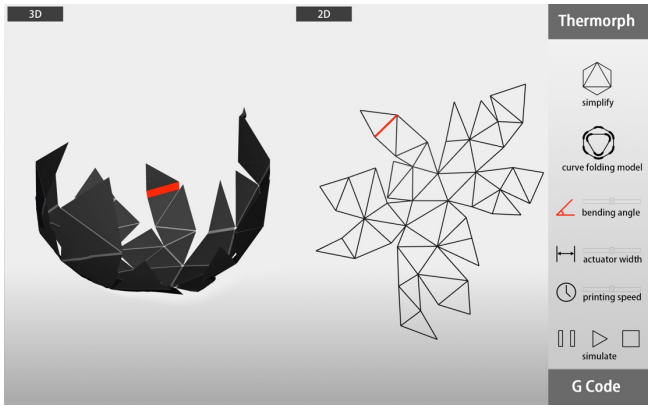

Figure 9. Thermorph editor: an interactive web-based design, visualization and simulation tool.

An interactive web-based design platform is developed to help with the design, simulation and fabrication of Thermorph structures (Figure 9). The end-to-end pipeline allows users to start with a 3D model or 2D pattern, and end with a printed sheet that can self-fold into a desired 3D shape upon heating.

The underlining pipeline is composed of five modules. Modeling, compiling and simulating modules are the backbones, while interactive editing and visualization modules provide the actual design environment. Our deterministic geometry algorithm providing mathematically guaranteed machine codes allows users to focus on the designs rather than hypothesize the right composite geometry for a desired transformation type.

Borrowing the design concept of inverse and forward kinematics in robotics [3], we include two design flows: inverse and forward design flow. While the inverse design flow helps users who already have a desired 3D shape to fold into, the forward design flow enables users to define the folding angles and explore the possible folded shape before they finalize their design.

Inverse Design Walkthrough

In this process (Figure 10), our steps start by (a) importing a desired 3D model that we hope to print flat; (b) simplifying the mesh into a sharp folding origami model, the input mesh is simplified into a desired number of mesh faces; (c) unfold the mesh, which can be unfolded into a 2D origami pattern, each edge is associated with a fold angle and a fold sequence information; (d) converting the sharp folding origami pattern into a curved folding origami pattern, and this step integrates the actual Thermorph actuator mechanisms; (e) simulating folding, thus we can simulate how the 2D pattern can be folded back into the original simplified 3D mesh; (f) generating the printing toolpath, the G-Code, contains information of the actuator geometry on each folding hinges, printing toolpath, printing speed, material options and other printing parameters on each layer; (g) printing the flat composite sheet; finally (h) triggering the self-folding with heat (hot water in this case).

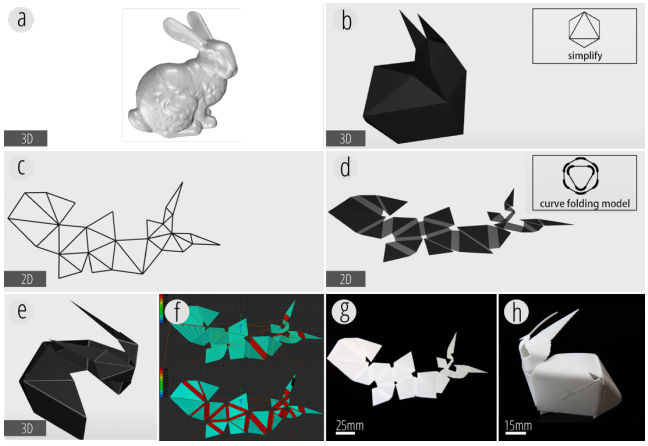

Figure 10. Inverse Design walkthrough to create the self-folding Stanford bunny.

Forward Design Walkthrough

In this design process (Figure 11), instead of importing a 3D mesh, our steps start by (a) importing a 2D pattern with the desired folding hinge location, and select each hinge to define the desired folding angle; (b) simulating folding in real-time simultaneously with Step a, thus user can obtain real-time feedback on the final folded shapes; (c) adjusting the selected actuator length, while keep the folding angle consistent, which is to give users more flexibility to adjust the bending curvature from a sharp fold to a curved bend, and printing speed will be adjusted accordingly; (d) simulating the folding of the entire pattern; (e, f, g) follow the same steps of the inverse design flow.

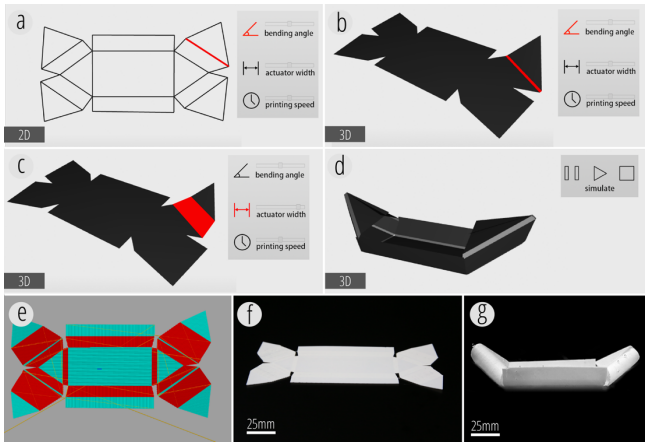

Figure 11. Forward design walkthrough to create a self-folding boat.

THERMORPH PIPELINE

Thermorph pipeline is a general design algorithm compiling an arbitrary 3D geometry into head motions of a 3D printer in G-Code format. Figure 12 shows an overview of the pipeline with a pyramid as an example, composed of one square and four equilateral triangles.

Step 1: Mesh Preparation for A Selected 3D Printer

This step adjusts a given geometry and make it suitable for a target 3D printer. The output is a *pre-processed mesh* $M=(V, F, p)$, where *vertex* v is in the *vertex set* V, a *face* (v_1, v_2, ... v_t) is a polygon with t vertices in the *face set* F, and $p(v)$ is a coordination in a 3D space ($\mathbb{R}^3$) associated to *vertex* v. For example, the Stanford Bunny in Figure 10a is a given mesh. Figure 10b shows the adjusted Stanford Bunny for printing by simplification and scale filters of Meshlab [4].

Step 2: Unfold Mesh and Calculate Fold Angles

This step outputs *development* $D=(V, F, q, \theta)$, which is an unfolded mesh with fold angle information (Figure 12b). For this step, we reuse algorithms [1, 32] that unfold a mesh and calculate the fold angles. Vertex set V and face set F are from the input mesh, and $q(v)$ is the unfolded coordination of vertex v on a plane ($\mathbb{R}^2$). $E(F)$ is the *edge set* containing *fold line* $e \in E(F)$; the *fold line* is defined by the intersection of the faces and is associated to the fold angle $\theta(e) \in [-\pi, \pi]$ (Figure 12a). Depending on whether it is greater or smaller than 0°, it represents either a valley fold or a mountain fold. The fold angle between the square and the triangle is

$$\theta = \pi - \arccos\frac{1}{\sqrt{3}} \cong 2.2 \text{ radians } (126.1°).$$

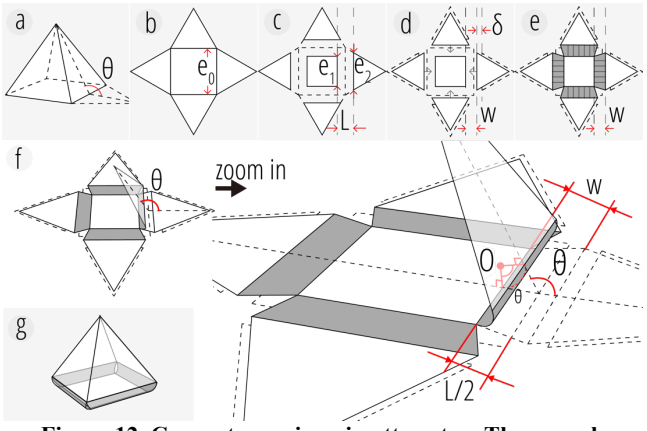

Figure 12. Convert an origami pattern to a Thermorph printing pattern. (a) folded states of the development, (b) unfolded states of the development (a net representing traditional origami) (c-e) Converting process. (e) The thin lines of four actuation areas represent the direction of the curve, when it is triggered. (f) The curve origami model folds on its actuator. The angle of arc O is equal to the fold angle θ. (g) Thermorph's 3D geometry- the curved origami model, which is (e)'s self-folded geometry.

Step 3: Build Curve Origami Model

Step 3 is to compile a development (Figure 12b) representing the 3D geometry (Figure 12a) to a *curved origami model* (Figure 12e) representing Thermorph's 3D geometry (Figure 12g).

Thermorph's *curved origami model* is based on a uniform shrinking material model. According to our experimental results shown in Figure 6 and 7, printing speed determines the arc of an actuator with radius r. For the fold angle θ of a given development (Figure 12a, f), a unique arc (with r) exists as shown in Figure 12f. The distance of two ends along the curve is W (Figure 12f). The width W of the unfolded actuator (Figure 12f) is determined by r and θ:

$$W = r\,|\theta|.$$

To locate the faces of the curved origami model, our algorithm solves the reduction length L and shifting distance δ, with the determined gap distance W

$$L - \delta = W.$$

Because the angle θ of arc O and fold angle θ are the same, the reduction length L is

$$L = 2 \cdot \left(\frac{L}{2}\right) = 2 \cdot \left(\tan\frac{\theta}{2} r\right).$$

The shifting distance is δ

$$\delta = L - W = 2 \cdot \left(\tan\frac{\theta}{2} r\right) - r|\theta|.$$

After solving the reduction length L and shifting distance δ, the algorithm reduces the size of two adjacent faces by moving the outlines (Figure 12c). The reduced length of each polygon is $\frac{L}{2}$. The moved outline changes the edge lengths of the faces. If e_0 denotes the origional edge length, the reduced square's edge length is $e_1 = e_0 - 2 \cdot (\frac{L}{2})$ and the reduced triangle's edge length is $e_2 = e_0 - 2 \cdot (\frac{L}{2}) \cdot \sin\frac{\pi}{6}$. Next, the faces are shifted by the shifting distance δ (Figure 12d). Finally, the algorithm inserts a trapezoid-shaped actuator with the gap distance, as shown in Figure 12e. Algorithm 1 shows the details of the actuator insertion.

Algorithm 1: Compile Curved Origami Model

Input: Development (V, F, q, θ).
Output: Curved origami model (V', F', C, q')

(1) For each edge $e = (a, b) \in E(F)$, such that e is between two faces, f_1 and f_2.
  (a) Add new point $q'(a)$ and $q'(b)$ by copying $q(a)$ and $q(b)$, respectively.
  (b) Replace vertices a, b of f_2 to new vertices a', b', respectively.
  (c) Add new point $q'(a')$ and $q'(b')$ by copying $q(a)$ and $q(b)$, respectively.
  (d) Insert new actuator $c=((a, b), (b', a'))$ into actuator set C.
  (e) Shift edge (a, b) and (a', b') with $L/2$ (Figure 12c).
  (f) Shift face f_2 and all connected faces with δ (Figure 12d).
(2) Output modified pattern as a curved origami model.

Step 4: Generate G-Code for Printing

The last step is to convert the printing pattern into G-Code. Considering that the bending direction is the same as the printing direction, when printing the actuator (the folding area), the toolpath should be perpendicular to the edges of the connected faces. While for faces between actuators, the printing direction does not matter. In addition, to strengthen the connections between actuators and faces, we print the PLA layers of the actuator 1mm longer on both sides

connected to adjacent faces, so that there is a 1mm overlap for bonding.

APPLICATION

We will detail four potential self-folding structures that can be manufactured by Thermorph.

Art - Self-folding Rose

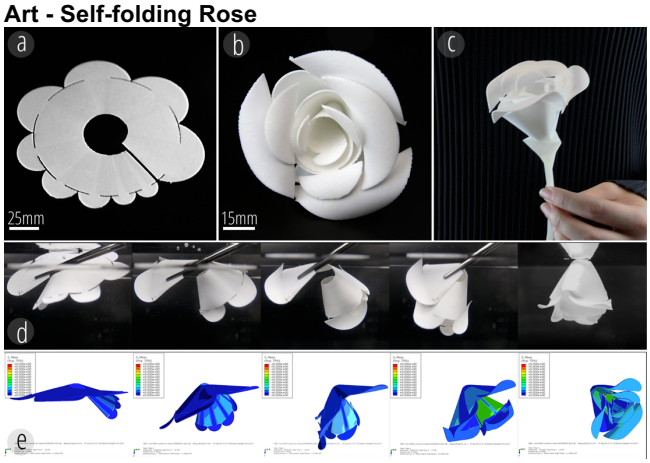

Figure 13. Self-folding rose: (a) a 3D printed flat sheet (16x14.5cm); (b) 3D rose after self-folding; (c) decorative rose as an art piece; (d) the sequential self-folding steps of the rose; (e) simulation of the self-folding steps.

We created a rose to illustrate a sequential deformation mechanisms in Thermorph system. Using forward design in the software editor, we improved the pattern design iteratively to achieve a rose shape with a spiral stem and several petals from one flat piece (Figure 13d). However, to improve the aesthetic quality, we refined the geometry once we verified the basic mechanisms in Thermorph editor. We design the structure to allow the fold of the vertical stem part in a spiral direction, followed by the flipping motion of each petal. The folding angle can be computationally controlled by printing speed and the width of the actuators, which is simulated in a finite element model (Figure 13e).

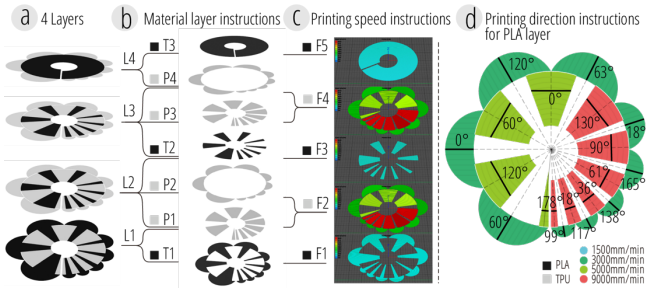

Figure 14. The fabrication method of the rose: (a) four printing layers (L1-L4), 0.2mm thickness for each; (b) each layer is printed with PLA (P1-P4) and TPU (T1-T3) composite, the thickness of P1, T2 and P4 is 0.4mm, others are 0.2mm. The layers can be organized into 5 printing files (F1-F5) for printing nozzle exchanges; (c) the printing tool path; (d) the printing direction and speed of the actuator layers matter.

Figure 14 shows the material configuration and printing methods of each layer. The level of complexity makes the automated design tool necessary.

Transportation - Self-Folding Boat

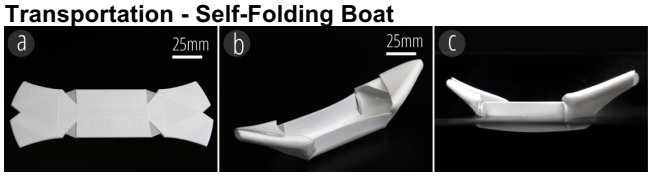

Figure 15. Self-folding boat: (a) a printed flat sheet (17.1x7.4cm); (b) a self-folded boat in 3D; (c) the boat can self-fold and float on a hot water surface.

Boat is another example for us to test out the forward design procedure in Thermorph editor as this example starts with a 2D pattern design as well (Figure 15). Users fold and simulate each hinge in the software to determine the desired folding state. In addition, through this example, we envision that transportation tools can be self-assembled on site. The boat we designed self-folded on the surface of hot water of 70 °C. We can imagine a larger boat folds up on top of a natural hot spring.

Furniture - Self-Folding Chair

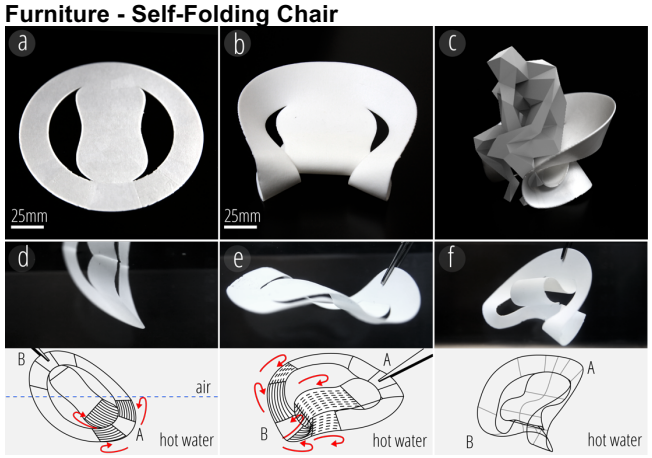

Figure 16. Self-folding chair: (a) a printed flat sheet (14x14cm); (b, c) a 3D chair after self-folding; (d-f) the sequential folding steps. The chair is soft when heated and solidifies when it cools down.

Flat pieces of furniture can save shipping and packaging cost, and provide convenience for transportation. With this self-folding chair design (Figure 16), we envision the scenario of "baking a chair" - flatly packed IKEA piece can be baked into a chair, when no assembly is needed.

Wearables - Self-Folding Armor

Unlike the previous applications that start with a flat pattern design, this armor starts with a 3D model (Figure 17a). We use the inverse design procedural in Thermorph editor for this case. We envision a self-assembling armor that can be put on top of a human body by itself (Figure 17b-d). In addition, the armor can be ironed flatly for easy carrying, and self-fold into 3D when heated again. This process is

reversible due to the shape memory effect of the thermoplastic (Figure 17e).

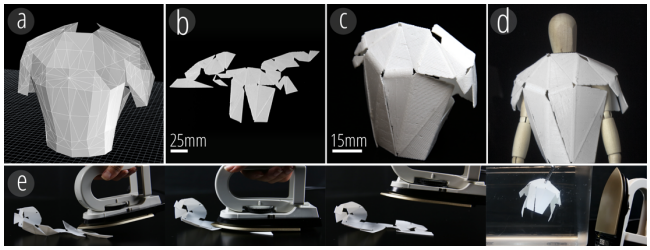

Figure 17. Self-folding armor: (a) a target 3D model; (b) a printed flat sheet (21.5x12.1cm); (c-d) a 3D armor after self-folding; (e) shape memory - the armor can be ironed flatly for easy carrying, and self-fold into 3D when heated again. This process is reversible.

Performance and Discussion

Reproducibility: Five rose printed (Figure 18) show an acceptable reproducibility of our technique. To ensure a high reproducibility, we will need to ensure the consistent printing and triggering conditions, including the heating temperature and time, the angle and fixed face during folding, and the speed of retrieval.

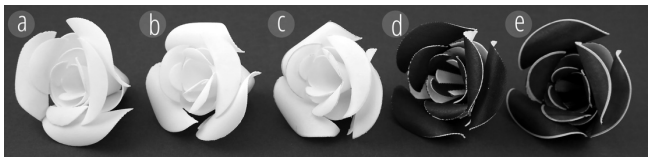

Figure 18. Five roses printed by Thermorph show a good reproducibility. Triggering temperature was 70°C, heating duration was 15 seconds. *Mismatch.*

The major reason for mismatching between the simplified 3D mesh and the printed model is gravity. To mitigate the influence, we chose the relatively centered face as the fixed face during the folding process, or purposely modified the printing speed from the theoretical calculation. For example, for the polyhedron in Table 1f, we have to fix the center face and place the whole structure in a way that all the hinges around the center face fold downwards for the ideal performance.

Mechanical strength: our current 1:100 chair is 0.8mm in thickness and can hold ~350g vertical load with < 5° elastic deformation. If our chair is modeled as a cantilever beam, for a 1:1 model that is capable of holding 50kg with 2° deformation, our calculation gives a ~3mm thickness requirement. We have conducted a preliminary test, with a 3mm strip with promising folding performance.

Collision: as the bunny (Figure 10) had one collision on the right of the neck, we orient it in a specific position to introduce some gravity effect to slow down the folding of the colliding faces; since the rose (Figure 13) collides if the outer petal folds faster than the inner ones, we fix the outermost petal during the folding process. In the future, we will explore additional features in our software to suggest the holding place and orientation during the folding process.

Scale: In the application examples, all cases except the rose were scaled down to fit the bed. Within the range of 25 - 225 cm^2, in our primitive and application cases experiments, scales do not have a substantial effect. In the future, we will explore the scale effect both in experiments and simulation.

Future Design Vision

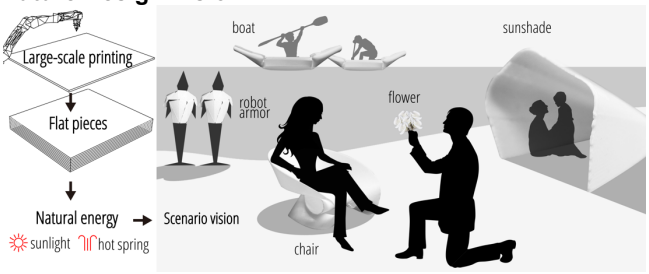

Figure 19. Design vision: self-assembly in the wild.

We envision an on-site fabrication scenario, where we print flat pieces and trigger them to self-assemble in the wild with natural energy - concentrated sunlight, hot springs, etc. For remote locations such as deserts where transporting large 3D structures is challenging, such technology becomes very relevant. The fact that we can choose engineering-graded ABS and Nylon material make this vision possible (Figure 19). Today in Africa, people make solar oven to bake pizza with mirror concentrated sunlight. We could use a similar setup to guide the self-folding process (e.g. a self-folding solar oven baked by a solar oven).

RELATED WORK

Faster Prototyping with Novel Digital Fabrication

A majority of 3D printers are still slow to even print a reasonably sized object. Researchers have introduced novel fabrication techniques to speed up the fabrication for prototyping physical artifacts: Platener to substitute some 3D prints with laser-cut plates [2], faBrikation to integrate construction kits into 3D prints [21], LaserOrigami [20] and LaserStacker [38] to utilize laser cutting and welding to create self-folding and layer stacking objects, and WirePrint [19] and WeaveMesh [34] to replace 3D surface with a wireframe mesh. HotFlex, in particularly, explored the manipulation of 3D printed PCL parts when they are heated above PCL T_g, for the purpose of saving fabrication time by printing pieces flatly [13]. However, the active transformation, or shape memory effect of thermoplastic is not discussed in the paper.

In terms of fast prototyping through folding, Foldio [23] introduced a software interface that can unfold a 3D paper origami model and suggest the 2D pattern that can be printed out of an inkjet printer. Foldio developed an actuation hinges, by attaching 3M tape on top of an inkjet printed heating trace. On top of Foldio, Thermorph extended both the design tool and the actuatable hinge structures, to make mostly arbitrary 3D mesh unfoldable, precise angle folding controllable, and thermoplastic based mechanically strong origami possible via 3D printing. In

addition, folding has been investigated as a mean for interaction [16], or as tangible input devices including Sketch-a-TUI [42], pop-up books [27] and interactive paper devices [30].

Shape Changing and Shape Memory Materials in HCI

There are three types of shape memory materials: shape memory polymer, shape memory alloy (SMA) and shape memory ceramic [17]. Shape memory alloy have been widely explored for HCI uses, including animated paper by Qi, et al [26], Shutter [5, 6] and much related work. SMA is conductive and has a high energy density, however, the form factor cannot be easily modified as it has a very high melting point. Comparing to shape memory alloy and ceramic, shape memory polymer tends to have the following advantage: a big variety of polymer material options; easy manipulation in form factor: fiber, spring, sheets, foam, other arbitrary 3D shapes; easy processing and programming.

Other shape actuation materials introduced in HCI include bi-strip thermoplastic material [15], pneumatic driven shape changing interfaces [24, 25, 29, 44], biological materials [41, 45] and digital materials enabled by electro-magnetic motors [10, 22]. Most of these materials have specific use cases, and requires customized fabrication process or customized 3D printing platform. For example, both biologic [45] and aeroMorph [24] require customized digital fabrication platform. In addition, except uniMorph [15], most of the shape changing materials are non-plastic based. We are interested in building on top of existing knowledge on shape control, and develop printable thermoplastic composite with commercial desktop FDM printers. We hope Thermorph add unique contributions to a bigger family of shape changing materials in HCI.

Shape Memory Thermoplastic for Self-Folding

Among the most relevant previous work, there are self-folding sheets with local light absorption [1, 36], sequential self-folding polymer sheets [2], and 3D printed self-folding composite with low-cost 3D FDM printers [38]. Using the same polymer sheets, researchers equipped the sheets with an additional conductive layer for joule heating for robotic applications and programmable self-folding structures [8, 9]. Similar to our technique, all these works are based on the prestress/prestrain that were embedded in the polymer; the reheating of the polymer causes the release of the prestress and the shrinking of the polymer. However, the polymer used in some of the previous work [1, 2, 35] is off-the-shelf product - Shrinky Dink (purchased from Amazon); it is uniformly pre-stressed, and a one-layer structure that has to be added with either an ink-jet printed pattern or a conducting heating pattern in order to be foldable. In contrast, our technology focuses on the development of a bi-layer structure, with each layer has a differential pre-stress and Young's modulus.

Comparing with the work by Manen at al [39] that has achieved angle control for various geometries via FDM printing, the major contribution our work is that we use printing speed as the major variable to control bending angles, whereas the previous work [38] suggested that the effect of printing speed is negligible. Although they listed some factors affecting bending angles, including layer height, actuator thickness and nozzle temperature, none of these was used to tune bending angles in their design. Our analysis is that these parameters are hard to be constantly varied within one continuous print. Instead, for the cube and dodecahedron requiring precise angle control in [38], angled grooves were printed at the hinges. However, printing resolution limits the minimum size and thickness of the grooves, which further limits the number and minimum thickness of faces within one sheet. In addition, different from the single-material option (PLA) introduced in [38], we use a PLA-TPU composite. As TPU has a lower tensile modulus (~25 Mpa) than PLA at its T_g (~350Mpa), our composite is more rigid and retains a more stable shape when heated.

In terms of adapting 3D printing techniques for thermoplastic-based self-folding structures, FDM 3D printed pre-stressed polymer was discussed before [46, 47]. However, they only talked about single material printing with the thin-wall structure for meta-material design; they have not talked about composite self-folding structures with multiple polymers involves. With multi-jetting and photocurable printing techniques, fiber-matrix based composite for self-folding was test [11]. However, this requires customized photo-curable resin and hacking a high-end 3D printer such as Objet260 Connex3 (Stratasys).

Self-Folding and 4D Printing

Beyond heat triggered shape memory thermoplastic, other materials responding to other stimuli can be printed and self-fold as well. These systems are in general called self-folding materials, self-assembly materials, or 4D printing [35]. Many stimuli responsive phenomena have been used for 4D printing including hygroscopic materials [45], swelling behavior of hydrophilic materials [7, 12], glassy shape memory polymer fibers in an elastomeric matrix [11], synthesized six UV-curable materials [32], etc. Comparing with our technique, these response to different stimuli and for most of the cases, they require very customized materials that are specifically synthesized and high end or self-customized printers.

CONCLUSION

In this paper, we presented Thermorph, a rapid prototyping system through self-folding mechanisms of shape memory thermoplastic. While self-folding has been introduced for manufacturing, the main contribution of this paper is to introduce a novel composite material design, a low cost FDM 3D printing approach, and an end-to-end design pipeline to fold a variety of arbitrary 3D geometries from a flat sheet.

While our approach has proved to save printing time and post-processing efforts for a lot of complex 3D geometry

fabrication comparing to standard 3D printing approach, we see the main promise of the work to achieve novel folding structures with readily available printing materials. For future work, we plan to go beyond desktop 3D printers and explore such self-folding structures on a larger scale.

ACKNOWLEDGEMENTS

The authors thank Guanyun Wang, Chengyuan Wei, as well as D. Damian, E. Demaine, M. Demaine, E. Groban, Y. Ke, J. Ku, F. Mazzoldi, S. Miyashita, C. Olguin, J. Ou, L. Peck, C. Sung, D. Rus, M. Tolley, S. Tibbits, C. Venter, and S. Woo for insightful discussions.

name	specification	printing layer instructions	actuator layer instructions	before heating	self-folding in progress	after heating
(a) Straight Fold	Actuator #: 1, Case A PLA orientation: 0° Printing speed of PLA: 5000mm/min					
(b) Angled Fold	Actuator #: 1, Case A PLA orientation: 45° Printing speed of PLA: 5000mm/min	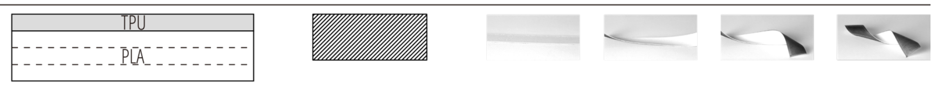				
	Actuator #: 3, Case A PLA orientation: 135°, 45°, 135° Printing speed of PLA: 5000mm/min					
	Actuator #: 4, Case A PLA orientation: 0°, 90° Printing speed of PLA: 5000mm/min	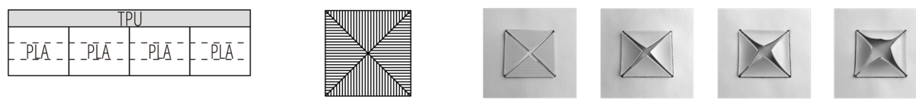				
(c) Two-side Fold	Actuator #: 5, Case A & Case B PLA orientation: 0° Printing speed of PLA: 5000mm/min	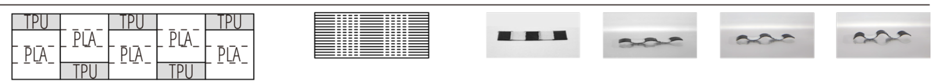				
	Actuator #: 6, Case A & Case B PLA orientation: following the curve Printing speed of PLA: 5000mm/min	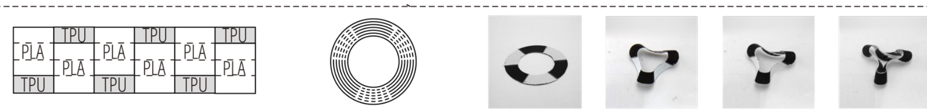				
(d) Circular Fold	Actuator #: 1, Case A PLA orientation: following the curve Printing speed of PLA: 5000mm/min Trigger T: 70°C					
	Actuator #: 1, Case A PLA orientation: following the curve Printing speed of PLA: 5000mm/min Trigger T: 70°C					
	Actuator #: 1, Case A PLA orientation: following the curve Printing speed of PLA: 5000mm/min Trigger T: 70°C					
(e) Polygonal Fold	Actuator #: 2, Case A PLA orientation: 0° Printing speed of PLA: 5000mm/min Trigger T: 80°C	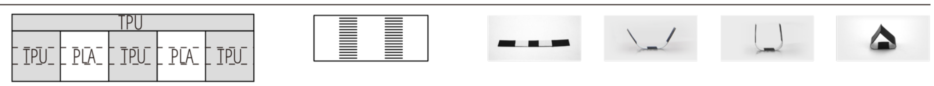				
	Actuator #: 3, Case A PLA orientation: 0° Printing speed of PLA: 5000mm/min Trigger T: 80°C	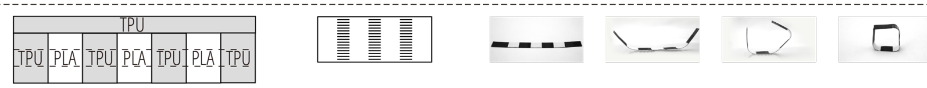				
(f) Polyhedron Fold	Actuator #: 3, Case A PLA orientation: 30°, 90°, 150° Printing speed of PLA: 9000mm/min Trigger T: 70°C					
	Actuator #: 5, Case A PLA orientation: 0°, 90° Printing speed of PLA: 9000mm/min Trigger T: 70°C	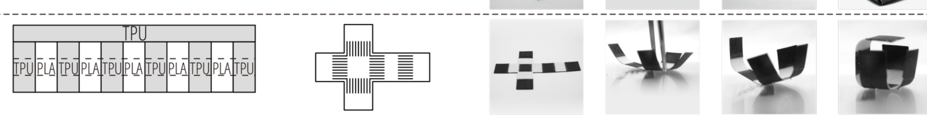				
	Actuator #: 7, Case A PLA orientation: 0°, 60°, 120° Printing speed of PLA: 9000mm/min Trigger T: 70°C	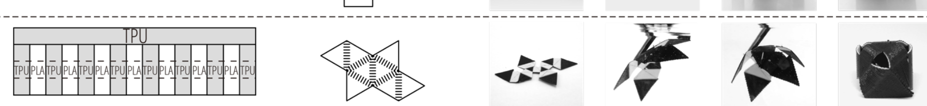				
	Actuator #: 19, Case A PLA orientation: 0°, 60°, 120° Printing speed of PLA: 9000mm/min Trigger T: 70°C	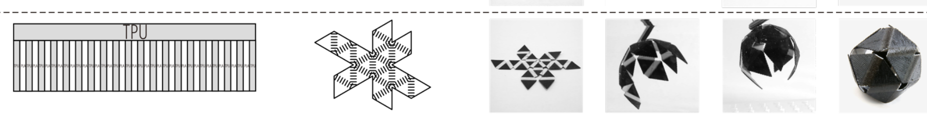				

Table 1. Geometric primitives.

REFERENCES

1. An, B., Miyashita, S., Tolley, M.T., Aukes, D.M., Meeker, L., Demaine, E.D., Demaine, M.L., Wood, R.J., Rus, D. 2014. An end-to-end approach to making self-folded 3D surface shapes by uniform heating. In *Proceedings of the 2014 IEEE International Conference on Robotics and Automation (ICRA)*, 1466-1473.
2. Beyer, D., Gurevich, S., Mueller, S., Chen, H.-T., Baudisch, P. 2015. Platener: Low-fidelity fabrication of 3D objects by substituting 3D print with laser-cut plates. In *Proceedings of the CHI 2015*, 1799-1806.
3. Carneiro, O., Silva, A., Gomes, R. 2015. Fused deposition modeling with polypropylene. *Materials & Design 83*, 768-776.
4. Cignoni, P., Callieri, M., Corsini, M., Dellepiane, M., Ganovelli, F., Ranzuglia, G. 2008. Meshlab: an open-source mesh processing tool. In *Proceedings of the Eurographics Italian Chapter Conference*, 129-136.
5. Coelho, M., Ishii, H., Maes, P. 2008. Surflex: a programmable surface for the design of tangible interfaces. In *Proceedings of the CHI'08 extended abstracts on Human factors in computing systems*, 3429-3434.
6. Coelho, M., Maes, P. 2009. Shutters: a permeable surface for environmental control and communication. In *Proceedings of the TEI 2009*, 13-18.
7. Correa, D., Papadopoulou, A., Guberan, C., Jhaveri, N., Reichert, S., Menges, A., Tibbits, S. 2015. 3D-Printed Wood: Programming Hygroscopic Material Transformations. *3D Printing and Additive Manufacturing 2*, 106-116.
8. Felton, S., Tolley, M., Demaine, E., Rus, D., Wood, R. 2014. A method for building self-folding machines. *Science 345*, 644-646.
9. Felton, S.M., Tolley, M.T., Onal, C.D., Rus, D., Wood, R.J. 2013. Robot self-assembly by folding: A printed inchworm robot. In *Proceedings of the 2013 IEEE International Conference on Robotics and Automation (ICRA)*, 277-282.
10. Follmer, S., Leithinger, D., Olwal, A., Hogge, A., Ishii, H. 2013. inFORM: dynamic physical affordances and constraints through shape and object actuation. In *Proceedings of the UIST 2013*, 417-426.
11. Ge, Q., Qi, H.J., Dunn, M.L. 2013. Active materials by four-dimension printing. *Applied Physics Letters 103*, 131901.
12. Gladman, A.S., Matsumoto, E.A., Nuzzo, R.G., Mahadevan, L., Lewis, J.A. 2016. Biomimetic 4D printing. *Nature materials 15*, 413-418.
13. Groeger, D., Chong Loo, E., Steimle, J. 2016. Hotflex: Post-print customization of 3d prints using embedded state change. In *Proceedings of the CHI 2016*, 420-432.
14. Hawkes, E., An, B., Benbernou, N.M., Tanaka, H., Kim, S., Demaine, E., Rus, D., Wood, R.J. 2010. Programmable matter by folding. *Proceedings of the National Academy of Sciences 107*, 12441-12445.
15. Heibeck, F., Tome, B., Della Silva, C., Ishii, H. 2015. uniMorph: Fabricating thin film composites for shape-changing interfaces. In *Proceedings of the UIST 2015*, 233-242.
16. Khalilbeigi, M., Lissermann, R., Kleine, W., Steimle, J. 2012. FoldMe: interacting with double-sided foldable displays. In *Proceedings of the TEI 2012*, 33-40.
17. Lendlein, A., Kelch, S. 2002. Shape-memory polymers. *Angewandte Chemie International Edition 41*, 2034-2057.
18. Liu, Y., Shaw, B., Dickey, M.D., Genzer, J. 2017. Sequential self-folding of polymer sheets. *Science Advances 3*, e1602417.
19. Mueller, S., Im, S., Gurevich, S., Teibrich, A., Pfisterer, L., Guimbretière, F., Baudisch, P. 2014. WirePrint: 3D printed previews for fast prototyping. In *Proceedings of the UIST 2014*, 273-280.
20. Mueller, S., Kruck, B., Baudisch, P. 2013. LaserOrigami: laser-cutting 3D objects. In *Proceedings of the CHI 2013*, 2585-2592.
21. Mueller, S., Mohr, T., Guenther, K., Frohnhofen, J., Baudisch, P. 2014. faBrickation: fast 3D printing of functional objects by integrating construction kit building blocks. In *Proceedings of the CHI 2014*, 3827-3834.
22. Nakagaki, K., Dementyev, A., Follmer, S., Paradiso, J.A., Ishii, H. 2016. ChainFORM: A Linear Integrated Modular Hardware System for Shape Changing Interfaces. In *Proceedings of the UIST 2016*, 87-96.
23. Olberding, S., Soto Ortega, S., Hildebrandt, K., Steimle, J. 2015. Foldio: Digital fabrication of interactive and shape-changing objects with foldable printed electronics. In *Proceedings of the UIST 2015*, 223-232.
24. Ou, J., Skouras, M., Vlavianos, N., Heibeck, F., Cheng, C.-Y., Peters, J., Ishii, H. 2016. aeroMorph-Heat-sealing Inflatable Shape-change Materials for Interaction Design. In *Proceedings of the UIST 2016*, 121-132.
25. Ou, J., Yao, L., Tauber, D., Steimle, J., Niiyama, R., Ishii, H. 2014. jamSheets: thin interfaces with tunable stiffness enabled by layer jamming. In *Proceedings of the TEI 2014*, 65-72.
26. Qi, J., Buechley, L. 2012. Animating paper using shape memory alloys. In *Proceedings of the CHI 2012*, 749-752.
27. Qi, J., Buechley, L. 2010. Electronic popables: exploring paper-based computing through an

interactive pop-up book. In *Proceedings of the TEI 2010*, 121-128.

28. Raviv, D., Zhao, W., McKnelly, C., Papadopoulou, A., Kadambi, A., Shi, B., Hirsch, S., Dikovsky, D., Zyracki, M., Olguin, C. 2014. Active printed materials for complex self-evolving deformations. *Scientific reports 4*, 7422.
29. Sareen, H., Umapathi, U., Shin, P., Kakehi, Y., Ou, J., Ishii, H., Maes, P. 2017. Printflatables: Printing Human-Scale, Functional and Dynamic Inflatable Objects. In *Proceedings of the CHI 2017*, 3669-3680.
30. Saul, G., Xu, C., Gross, M.D. 2010. Interactive paper devices: end-user design & fabrication. In *Proceedings of the TEI 2010*, 205-212.
31. Schmutzler, C., Zimmermann, A., Zaeh, M.F. 2016. Compensating warpage of 3D printed parts using free-form deformation. *Procedia CIRP 41*, 1017-1022.
32. Sundaram, S., Kim, D.S., Baldo, M.A., Hayward, R.C., Matusik, W. 2017. 3D-printed self-folding electronics. *ACS applied materials & interfaces 9*, 32290-32298.
33. Takahashi, S., Wu, H.Y., Saw, S.H., Lin, C.C., Yen, H.C. 2011. Optimized topological surgery for unfolding 3d meshes. In *Proceedings of the Computer graphics forum*, 2077-2086.
34. Tao, Y., Wang, G., Zhang, C., Lu, N., Zhang, X., Yao, C., Ying, F. 2017. WeaveMesh: A Low-Fidelity and Low-Cost Prototyping Approach for 3D Models Created by Flexible Assembly. In *Proceedings of the CHI 2017*, 509-518.
35. Tibbits, S., McKnelly, C., Olguin, C., Dikovsky, D., Hirsch, S. 2014. 4D Printing and universal transformation.
36. Tolley, M.T., Felton, S.M., Miyashita, S., Aukes, D., Rus, D., Wood, R.J. 2014. Self-folding origami: shape memory composites activated by uniform heating. *Smart Materials and Structures 23*, 094006.
37. Tumbleston, J.R., Shirvanyants, D., Ermoshkin, N., Janusziewicz, R., Johnson, A.R., Kelly, D., Chen, K., Pinschmidt, R., Rolland, J.P., Ermoshkin, A. 2015. Continuous liquid interface production of 3D objects. *Science 347*, 1349-1352.
38. Umapathi, U., Chen, H.-T., Mueller, S., Wall, L., Seufert, A., Baudisch, P. 2015. Laserstacker: Fabricating 3D objects by laser cutting and welding. In *Proceedings of the UIST 2015*, 575-582.
39. van Manen, T., Janbaz, S., Zadpoor, A.A. 2017. Programming 2D/3D shape-shifting with hobbyist 3D printers. *Materials Horizons 4*, 1064-1069.
40. Wang, G., Yao, L., Wang, W., Ou, J., Cheng, C.-Y., Ishii, H. 2016. xPrint: A Modularized Liquid Printer for Smart Materials Deposition. In *Proceedings of the CHI 2016*, 5743-5752.
41. Wang, W., Yao, L., Zhang, T., Cheng, C.-Y., Levine, D., Ishii, H. 2017. Transformative Appetite: Shape-Changing Food Transforms from 2D to 3D by Water Interaction through Cooking. In *Proceedings of the CHI 2017*, 6123-6132.
42. Wiethoff, A., Schneider, H., Rohs, M., Butz, A., Greenberg, S. 2012. Sketch-a-TUI: low cost prototyping of tangible interactions using cardboard and conductive ink. In *Proceedings of the TEI 2012*, 309-312.
43. Yang, W.G., Lu, H., Huang, W.M., Qi, H.J., Wu, X.L., Sun, K.Y. 2014. Advanced shape memory technology to reshape product design, manufacturing and recycling. *Polymers 6*, 2287-2308.
44. Yao, L., Niiyama, R., Ou, J., Follmer, S., Della Silva, C., Ishii, H. 2013. PneUI: pneumatically actuated soft composite materials for shape changing interfaces. In *Proceedings of the UIST 2013*, 13-22.
45. Yao, L., Ou, J., Cheng, C.-Y., Steiner, H., Wang, W., Wang, G., Ishii, H. 2015. BioLogic: natto cells as nanoactuators for shape changing interfaces. In *Proceedings of the CHI 2015*, 1-10.
46. Zhang, Q., Yan, D., Zhang, K., Hu, G. 2015. Pattern transformation of heat-shrinkable polymer by three-dimensional (3D) printing technique. *Scientific reports 5*.
47. Zhang, Q., Zhang, K., Hu, G. 2016. Smart three-dimensional lightweight structure triggered from a thin composite sheet via 3D printing technique. *Scientific reports 6*, 22431.